

Fracture characterization from scattered energy: A case study

Samantha Grandi K.[§], Sung Yuh[¶], Mark E. Willis[§], and M. Nafi Toksöz[§]

[§] Earth Resources Laboratory, MIT. Cambridge, MA.

[¶] Total Exploration & Production. Pau, France.

Abstract

We use 3D surface seismic data to determine the presence and the preferred orientation of fracture corridors in a field. The Scattering Index method is proving to be a robust tool for detecting and mapping fracture corridors. Fracture corridors largely control permeability and fluid flow in some fractured reservoirs. To apply the Scattering Index method, we compute the scattering transfer functions from the reservoir interval using prestack migrated data collected in four azimuth sectors. By measuring the azimuthal differences in the amount of scattering, we obtain maps of density of fracture corridors and their orientation across the survey area. We use geostatistical filtering to improve the spatial correlation of scattering index maps. The distribution and orientation of the final fracture corridors are interpreted considering the structure, fault network, and stress information. In the field, we observe several regions of high fracturing near the anticline's crest and on its steepest slopes, on the southwest flank. Around well locations, fractures are oriented to the NW and NNW, which agrees with estimates of maximum stress direction from well data.

1 Introduction

The objective of this study is to evaluate the potential of the Scattering Index method for characterizing a fractured reservoir. Our aim is to identify subsurface areas of high fracture density and estimate fracture orientation at the reservoir.

Well-developed methods for characterizing fractured reservoirs from seismic data examine converted waves, AVOA effects, and various seismic attributes (Pérez et al., 1999). In all these techniques, the effect of fractures on the wave propagation is described by an equivalent azimuthally anisotropic medium, presupposing that the size of the heterogeneity is smaller than seismic wavelengths.

The Scattering Index methodology attempts to extract fracture properties from the scattered waves, also known as coda waves, which are generated by fractures comparable in size to the seismic wavelength. In geology, such features are known as “fracture corridors” and have particular characteristics that distinguish them from discrete fractures and fault systems. Fracture corridors are zones of fracture clustering that extend several tens to hundreds of meters and consist of parallel, usually sub vertical fractures. Fracture corridors provide fluid flow paths; therefore, detecting their existence and extracting their properties is relevant in the assessment of fractured reservoirs.

2 The Scattering Index Method

Determination of fracture distribution and orientations using the Scattering Index method is based on the principle that fractures of dimensions similar to dominant seismic wavelengths, scatter energy, and that such signals have different character depending on the angle of observation. The Scattering Index method is relatively new (Willis et al., 2006). The method provides maps showing scattered energy associated to subsurface fracture corridors. It has been tested on synthetic 3D data generated with finite difference

approximations, and it has been applied successfully to field data where independent information about fractures exists.

Modeling studies on this phenomenon reveal that regularly spaced vertical fractures impart a ringing coda type of signature. Such signature varies in coherence and amplitude as a function of: 1) the angle between source-receiver line and fracture plane (strike); 2) the relationship between fracture spacing and dominant seismic wavelength; and 3) the compliance contrast between fracture and the surrounding medium. The numerical modeling experiments show that coda energy is most coherent parallel to strike of fractures and has its largest amplitude when the wavelength is tuned to fracture spacing and the fractures have low stiffness. During the course of processing, coda waves stack constructively when the acquisition direction is parallel to fractures and stack destructively normal to fractures.

The Scattering Index analysis consists of two steps. In the first step, azimuthal transfer functions of the fractured zone are obtained. Wavelets are extracted from zones above and below the reservoir level for each CDP in each stacked azimuth. Then, a transfer function is derived by deconvolving the corresponding upper wavelet from the lower wavelet. The method is intrinsically insensitive to overprinting since it looks for differences in the wavelet as a function of depth, as it crosses the reservoir.

Transfer functions exhibit the same attributes as the stacked coda waves: they ring and are less temporally compact in the direction parallel to fracture corridors. Given a 3D seismic set with a full range of azimuths, the particular character of transfer functions allows identification of fractured areas and determination of fracture strike. The second step consists of the calculation of the actual indices. The scattering index, SI , is a number that measures the 'ringiness' of the transfer function. It is defined in Willis et al. (2004), as:

$$SI = \sum_{i=0}^m |t_i| i^n \quad (1)$$

where i is the time lag, t_i is the transfer function amplitude at lag i (in the time domain), m is a lag at which there is no more significant energy in the transfer function, and n is an exponent, generally taken as one. Because this expression gives greater weight to the larger lags, the more the transfer function rings, the larger the value of SI , thus SI is the largest parallel to fractures.

3 The Field

3D seismic data were acquired and processed with the objective of obtaining an improved image of the reservoir. A sub-volume was selected for this and other anisotropy studies. The non-migrated gathers were rebinned with a 60 x 60 m bin size, and sorted into 4 azimuth limited sectors (figure 1) and offset range 0-500 m. This combination showed to be optimal in the sense of homogeneity on the fold distribution. 3D pre-stack Kirchhoff time migration was performed on each azimuth sector, prior to regridding, and the original full-stack post-processing sequence was applied to the migrated volumes.

This study used the four azimuth sector seismic cubes in which only the near offsets were stacked and had all pre- and post-migration processing applied (figure 2). In addition, we used the seismic interpretation of the top of the reservoir and basement horizons, and three well locations for geographical reference. The reservoir P-wave velocity is around 3100 m/s and the frequency bandwidth at this level is between 10 and 70 Hz, which implies that dominant wavelength is greater than 45 m. The individual and collective effects on the scattering signal, of the filters and processes applied to the seismic data, need to be studied further.

4 Results

After calculation of transfer functions and scattering indices for the top of the reservoir horizon, we determine the azimuth sector at which the scattering index has its maximum value for each CDP bin location. Figure 3 shows the direction with highest angular contrast in scattering index. Colors represent azimuths as in figure 1. White bins indicate where no sector is particularly dominant. Figure 3 shows the direct result of the Scattering Index method.

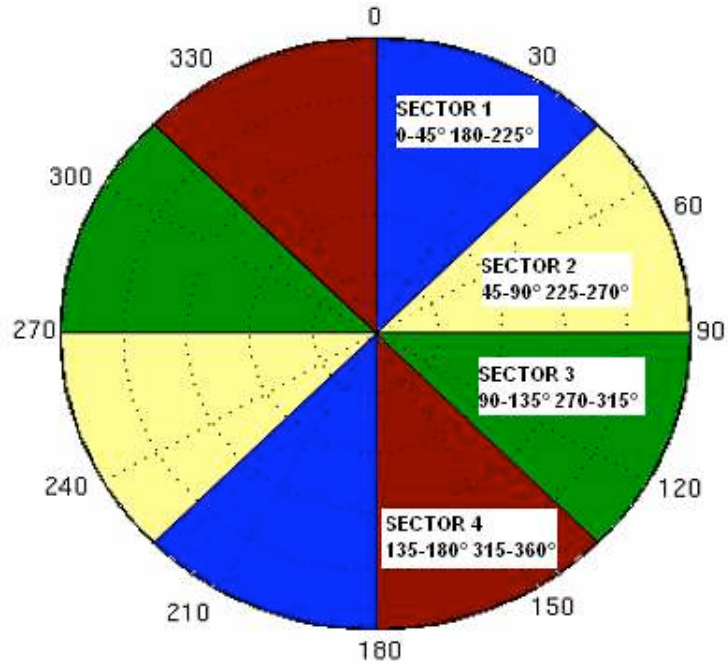


Figure 1: Convention of azimuthal sectoring

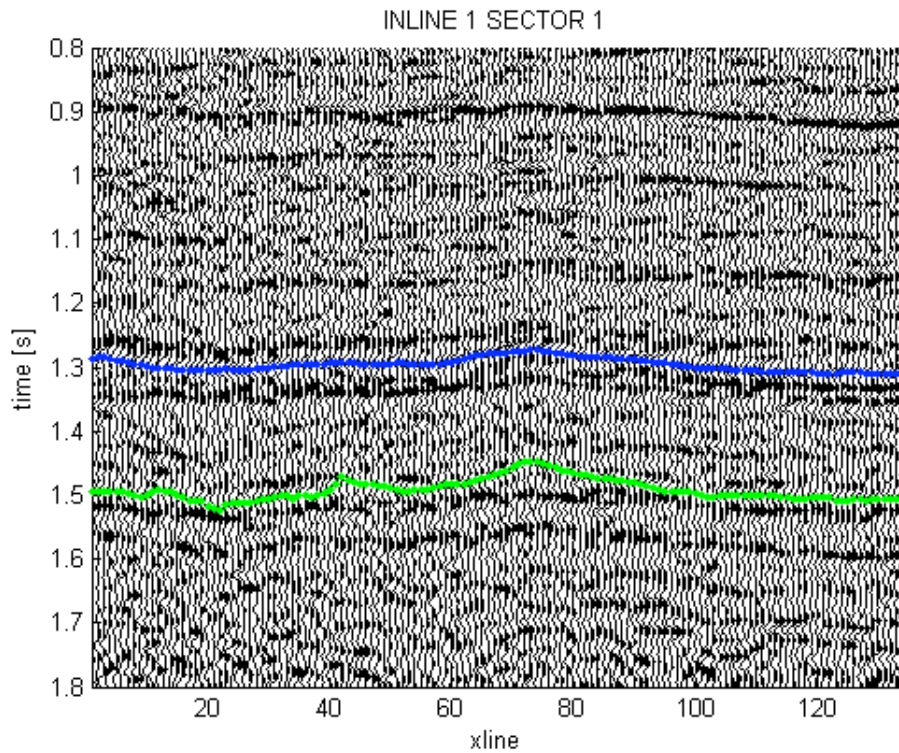


Figure 2: Typical seismic section in the field. Top of reservoir (blue) and basement (green) horizons.

A strong footprint component remains in the data, partly because only near offsets were stacked. A filtering technique is used to remove the footprint, which is based on Factorial Kriging, a geostatistical approach to isolate and extract features related to a modeled variogram (Yarus et al., 2003). The map of maximum scattering index values ignoring their orientation is analyzed for nugget, inline, and crossline effect, and filters are designed to remove them.

Figure 4 shows the filtered map, which represents the fracture distribution across the area of study. Regions of higher correlation, or continuity of data (darkest red), are interpreted as highly fractured areas. We then remove the footprint from each azimuth by applying the same filters to each azimuth map. Figure 5 shows the combined filtered map of azimuth sectors of maximum scattering index.

The results of fracture index analysis are shown with various degrees of detail in figures 4, 5, and 6. Looking at figure 4, around the well locations (366, 377, and 371), the Scattering Index method suggests that fracture corridors run NW-SE and NNW-SSE, which agrees with the regional maximum horizontal stress known for the area (N 140° E). In situ stress direction derived from induced fractures in image logs varies in the field and differs in some cases from the regional stress direction. In particular, Shmax is oriented N 170° E in well 366, N 140° E in well 371 and N 80° E in well 377.

Changes of fracture orientation are known to occur in the proximity of faults or in places where the topography of the reservoir is abrupt. In Figure 5, fracture orientation is compared to the fault interpretation. Two conjugate sets of faults, trending NW-SE and NE-SW, are predominant in the area. Some correlation between fault strikes and fracture orientations is observed; in the central region, fracture directions are parallel to the NW-SE faults, while at other regions both trends are observed.

Close to certain faults, for example, along fault number 7, fracture azimuth varies quite erratically. However, this fault separates two distinctly fractured blocks with opposite orientations. The region to the south of fault 7 has dominant fracture azimuth 45-90° (sector 2), whereas in the northern block, fractures are predominantly oriented in the conjugate direction (sector 4). There are other highly fractured regions where orientations vary rapidly, for instance, to the northeast of the survey area.

We compare in figure 6 the structure at the reservoir level with the scattering index result. Blue colors represent higher levels of the structure. The presumed axis of the anticline is also shown. The zone of no fractures extending north of well 371 and east of well 366 is precisely where the structure has the least dip. A fractured zone with dominant azimuth sector 3 extends for about 1 Km to the west of well 366 (indicated as A). Fractures in region A are sub-parallel to the anticline main axis (NW-SE). To the southwest of region A, a larger area of about 2.5 km², near well 377 (B), exhibits consistently azimuth sector 4 (NNW-SSE). Both of these zones are located on the west part of the area where dips are greater.

From figures 4 and 6, we note that, in average, the dominant direction of fracture corridors is nearly parallel to the axis of the anticline. Figure 6 shows that local variations do exist.

5 Conclusions

We apply the Scattering Index method to locate fracture corridors and their dominant direction in a field. Fracture distribution varies across the area. Low-density zones extend in a narrow band from the center to the north of the area, and on the northwest and southeast parts. Highly fractured regions are found close to the well locations and to the northeast and southwest of the area. The variation in orientations is explained in terms of the structure and the presence of faults with two dominant strikes, NW-SE and NE-SW. Around the well locations, fractures are mainly oriented NW-SE and NNW-SSE. The estimated orientation of fracture corridors agrees with regional and in situ maximum stress directions, and with the anisotropy axis derived from an independent study.

Resolution of fracture orientation in the field is limited to 45° due to data azimuth fold. Ideally, this type of study would benefit from densely sampled multi-azimuth multi-offset data. It remains for future projects to study the effects on the scattering energy of specific seismic data processes, as for example, seismic migration, and to develop an optimal processing sequence that preserves scattering energy.

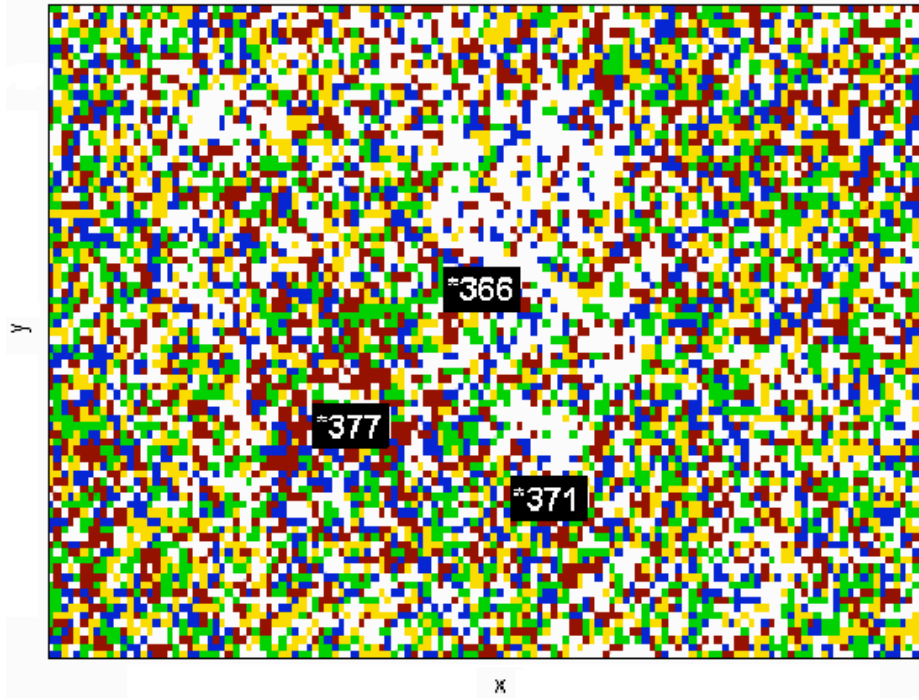


Figure 3: Azimuth sector of maximum scattering index. Color scale as in figure 1. Numbers designate the wells.

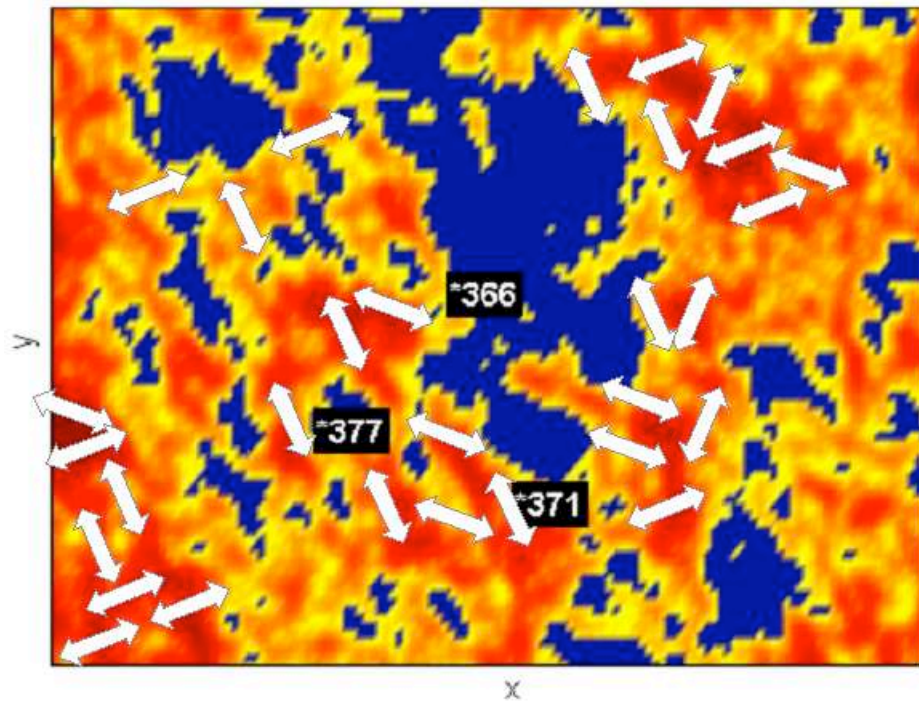


Figure 4: Fracture corridors density (colors) and orientations (arrows) in highly fractured regions.

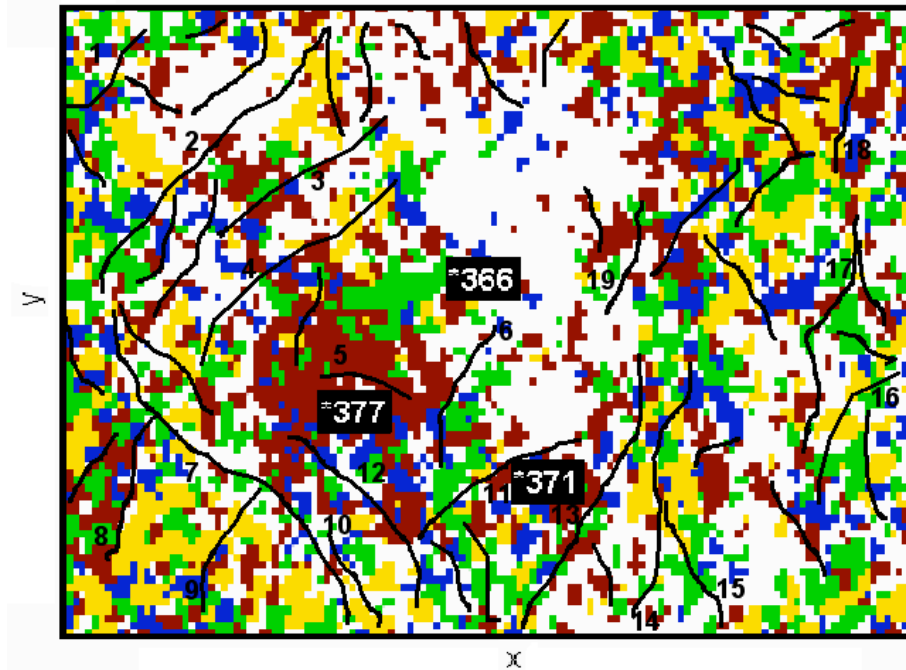


Figure 5: Azimuth sector of maximum scattering index (fracture corridors' orientations) after geostatistical filtering, and fault boundaries. Color scale as in figure 1.

6 Acknowledgements

The authors thank Total for giving permission to publish this study and providing the data. Stéphanie Legeron-Cherif, from ERMS, applied the geostatistical filter on the scattered index maps. We thank the Earth Resources Laboratory Founding Members for supporting this work.

References

- Pérez, M., Grechka, V., and Michelena, R. (1999). Fracture detection in a carbonate reservoir using a variety of seismic methods. *Geophysics*, 64(4):1266–1276.
- Willis, M., Burns, D., Rao, R., Minsley, B., Toksöz, N., and Vetri, L. (2006). Spatial orientation and distribution of reservoir fractures from scattered seismic energy. *Geophysics*. in press.
- Willis, M., Rao, R., Burns, D., and Byun, J. (2004). Spatial orientation and distribution of reservoir fractures from scattered seismic energy. In *Expanded Abstracts*. Society of Exploration Geophysicists, 74th Annual Meeting.
- Yarus, J., Chambers, R., and Guillaume, J. (2003). Identifying subtle stratigraphic and facies trends using advanced variography. AAPG, Annual Convention.

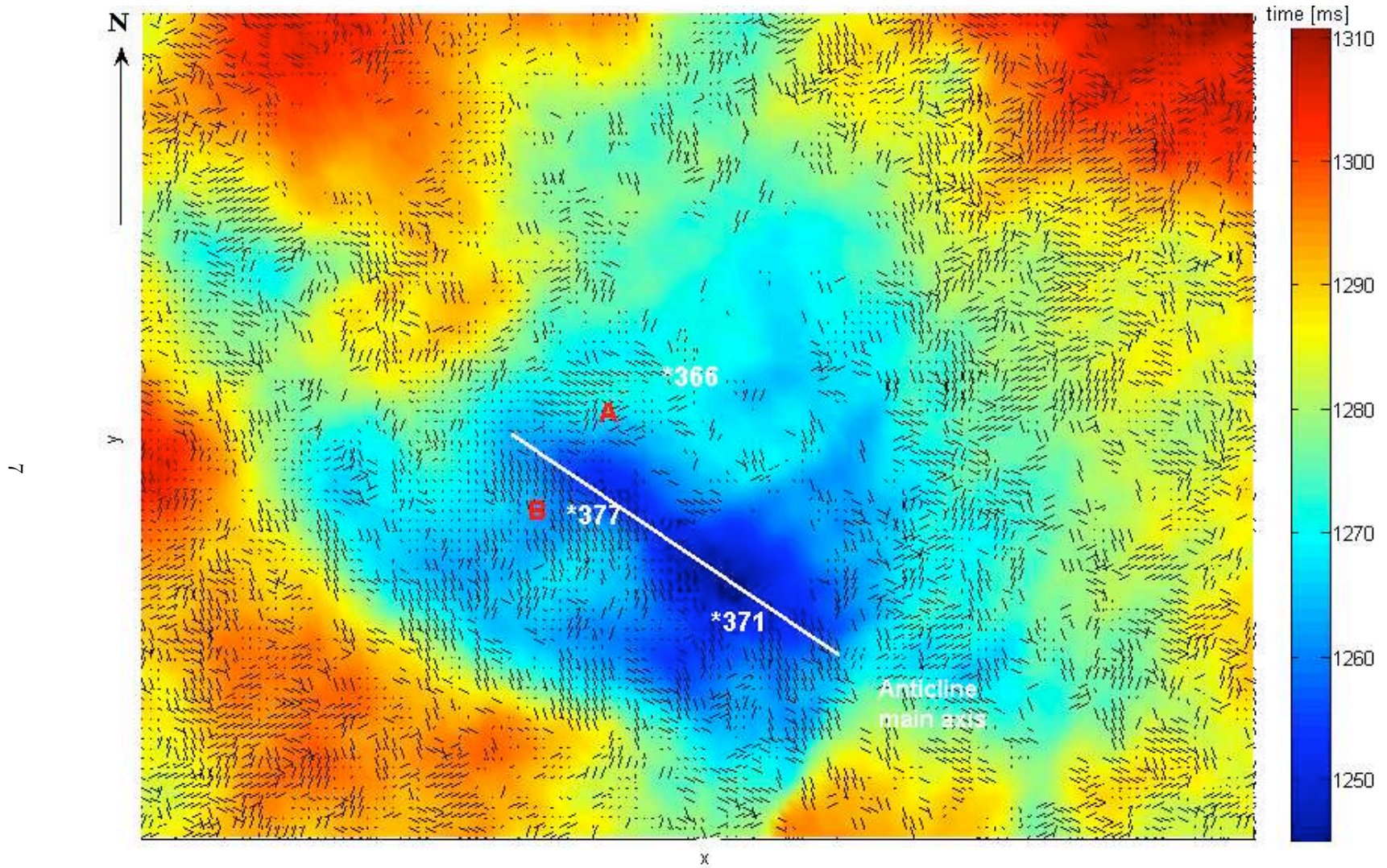


Figure 6: Structure at the reservoir level and fracture corridor orientations from the Scattering Index method (quivers).